Aging and Disease
www.aginganddisease.org
Early access date: December 5, 2025
http://dx.doi.org/10.14336/AD.2025.1130

Original Article

Islet Inflammation and Endocrine Function in Aging - Evaluating the Role of Toll-like receptor 4

Julia Jelleschitz[1], Annette Brandt[2], Klara Brehm[1], Vanessa Schnell[1], Tobias Jung[1], Ina Bergheim[2], Annika Höhn[1,3*]

[1]Department of Molecular Toxicology, German Institute of Human Nutrition Potsdam-Rehbruecke, Nuthetal, Germany. [2]Department of Nutritional Sciences, Molecular Nutritional Science, University of Vienna, Vienna, Austria. [3]German Center for Diabetes Research (DZD), München-Neuherberg, Germany.

[Received September 4, 2025; Revised November 29, 2025; Accepted November 30, 2025]

ABSTRACT: The aging process is accompanied by a gradual decline in tissue function, in part due to chronic low-grade inflammation that contributes to cardiovascular, neurodegenerative, and metabolic disease development. In the endocrine pancreas, Langerhans islets exhibit age-related structural and functional changes, including immune cell infiltration and fibrotic remodeling, as we recently demonstrated. Macrophages, as key immune mediators in both diabetic and aged islets, play a central role in Toll-like receptor 4 (TLR4) signaling, a pathway activated by bacterial lipopolysaccharides and known to exacerbate inflammation and tissue damage in multiple organs. We therefore hypothesize that TLR4 signaling contributes to the inflammatory changes during islet aging. To investigate this, two complementary mouse studies were performed. Aged C57BL/6J mice were treated with the TLR4 inhibitor TAK-242 for four months, which reduced insulitis, macrophage infiltration, and fibrosis, while preserving insulin secretion. In contrast, mice with a lifelong myeloid-specific deletion of TLR4 showed altered islet cell composition in young age, potentially leading to dysregulated insulin secretion, and signs of insulin resistance in aging, despite unchanged islet inflammation. These results indicate that TLR4 inhibition attenuates inflammatory islet remodeling in aging, whereas lifelong loss of myeloid TLR4 signaling seems to disrupt immune-endocrine interactions and impairs insulin secretion. Thus, TLR4-driven immune activation emerges as a mechanism linking inflammation to pancreatic islet aging.

Keywords: Aging, Langerhans Islets, Immune cells, TLR4, Fibrosis, Inflammation

INTRODUCTION

As the worldwide population age is steadily increasing, maintaining quality of life in the elderly is gaining increasing importance. The aging process is characterized by a decline in tissue function, influenced by various factors such as oxidative stress, inflammatory mediators or cellular senescence. These factors can lead to chronic low-grade inflammation, also referred to as "inflammaging" [1-3], promoting tissue dysfunction and contributing to the increased prevalence of cardiovascular, neurodegenerative or metabolic diseases, such as type-2-diabetes (T2D), a trend, that is expected to continue with demographic change [4, 5]. Various exogenous and endogenous factors such as obesity, physical inactivity and chronic inflammation are increasing the risk for T2D by promoting insulin resistance and β-cell dysfunction, ultimately leading to an inadequate response to glucose as a result of altered insulin secretion [6, 7].

Langerhans islets are a complex endocrine network embedded in the exocrine pancreas and play a central role in regulating insulin secretion and glucose homeostasis [8]. While β-cells are the main producer of insulin and numerically dominant, they interact closely with other endocrine cell types such as α-, δ-, and γ-cells as well as immune cells, pancreatic stellate cells and endothelial cells. During aging and T2D this complex network

***Correspondence should be addressed to:** Dr. Annika Höhn, German Institute of Human Nutrition, Potsdam-Rehbruecke (DIfE), Arthur-Scheunert-Allee 114-116, 14558 Nuthetal, Germany. Mail: annika.hoehn@dife.de.

undergoes structural and functional changes, including an increased number of immune cells as well as shifts of immune cell subtypes [9-11]. Interestingly, a limited and moderate increase in certain immune cell populations may improve glucose tolerance whereas excessive accumulation is generally associated with enhanced inflammatory signaling [10, 12].

Especially macrophages are known to accumulate in T2D islets and have been associated with elevated toll-like receptor (TLR) activation in diabetic animal models [13-18]. TLRs are pattern recognition receptors that detect distinct pathogen-associated molecular patterns and danger-associated molecular patterns and are highly expressed on immune cells, especially in macrophages. In total, 11 TLRs have been described in humans and 13 in mice, each recognizing specific exogenous microbial ligands or endogenous molecules [19, 20]. One of the most well-characterized is TLR4, which acts as homodimer, and primarily recognizes lipopolysaccharide (LPS), a cell wall component of gram-negative bacteria. TLR4 activation, together with its co-receptors, initiates inflammatory signaling cascades, leading to nuclear factor kappa-B (NF-κB) activation and interferon-regulatory factor (IRF)-mediated pathways. Indeed, elevated levels of bacterial toxins such as LPS and TLR4 activation have been shown to enhance inflammation, fibrosis and organ dysfunction, with the liver being one of the affected organs [21-24]. Similar mechanisms may contribute to pancreatic dysfunction during aging. In our recent study, we observed marked immune cell accumulation and fibrotic remodeling within aged Langerhans islets, pointing toward local inflammatory changes [10]. Given the known role of macrophages and TLR4 signaling in mediating tissue inflammation and metabolic dysfunction, we hypothesize that TLR4-driven immune activation contributes to age-associated structural and functional deterioration of pancreatic islets. To address this, two complementary mouse studies were performed: one using pharmacological TLR4 inhibition in aged C57BL/6J mice, and another employing a myeloid-specific TLR4 knockout model to assess the role of TLR4 signaling in pancreatic islets during aging.

MATERIAL AND METHODS

Animal procedures and study design

General animal care and ethics

All experiments complied with the European Directive 2010/63/EU, the National Institutes of Health guidelines for the care and use of laboratory animals, and site-specific institutional regulations described below. Mice were maintained under specific pathogen-free conditions in a controlled environment (20 ± 2 °C, 12:12 h light/dark cycle). At the University of Vienna, lights were on from 7:00 am to 7:00 pm; at the German Institute of Human Nutrition (DIfE), from 5:30 am to 5:30 pm. Animals had ad libitum access to standard chow (Ssniff, Soest, Germany) and water, unless otherwise specified.

Studies were conducted at two sites. At the German Institute of Human Nutrition (DIfE), Potsdam-Rehbruecke, Germany, all procedures were approved by the institutional animal welfare committee and the State Office for Environment, Health, and Consumer Protection of Brandenburg (approval no. 2347-46-2019). Animals used solely for tissue collection were euthanized in accordance with § 4(3) of the German Animal Welfare Act without additional authority approval. At the University of Vienna, Austria, all procedures were approved by the institutional ethics and animal welfare committee and the Federal Ministry of Education, Science and Research (BMBWF-2021-0.464.120, BMBWF-66.006/0014-V/3b/2019).

At the DIfE, animals were euthanized under anesthesia by acute isoflurane inhalation followed by cervical dislocation. At the University of Vienna, animals were euthanized under anesthesia by intraperitoneal (i.p.) ketamine (100 mg/kg) plus xylazine (16 mg/kg) followed by cervical dislocation and the collection of blood and tissue. Langerhans islets and quadriceps muscle tissue were isolated following cervical dislocation.

Age-comparative cohort: islet analyses, plasma endotoxin and pancreatic TLR4 ligands

Young (3-5 months) and old (19–26 months) C57BL/6J mice, bred in-house (Max Rubner Laboratory, DIfE), were used. Blood was collected by vena cava puncture for endotoxin quantification and pancreatic islets were isolated via liberase perfusion (see subsection Isolation of Langerhans islets) for gene expression analysis, single cell staining and *in vitro* LPS-stimulation experiments. In addition, whole pancreatic tissue was isolated and snap-frozen for the analysis of TLR4 ligands.

Pharmacological TLR4 inhibition in aged mice

Seventeen-month-old male C57BL/6J mice, bred in-house at the University of Vienna, received the TLR4 inhibitor TAK-242 (Cayman Chemical, USA; 0.3 mg/kg body weight (BW), i.p., twice weekly, on Mondays and Thursdays) or vehicle (0.1 % DMSO in NaCl) for 4 months. A glucose tolerance test (GTT) was conducted one week before sacrifice (see subsection Glucose tolerance test). At sacrifice, blood was collected from the portal vein, and pancreatic tissue was fixed in 4% formaldehyde and paraffin-embedded.

Myeloid-specific TLR4 knockout study

Male myeloid-specific TLR4 knockout mice ($Tlr4^{fl/LyzM\text{-}cre}$), generated by crossbreeding B6(Cg)-Tlr4^tm1.1Karp/J with B6.129P2-Lyz2^tm1(cre)Ifo/J, The Jackson Laboratory, USA) and age-matched wildtype (WT) $TLR4^{fl+/+LyzM\text{-}cre+/+}$ controls were bred in-house (University of Vienna). Young (4 months) and old (20 months) animals were included. One week before sacrifice, a GTT was performed (see subsection Glucose tolerance test). At sacrifice, blood was collected from the portal vein, pancreatic tissue was fixed in neutral-buffered formalin, and, in a subset, islets and quadriceps muscle were harvested for further analyses.

Age-comparative histology cohort

For additional immunohistochemical analyses, archived formalin-fixed pancreatic tissue from male C57BL/6J mice aged 3, 19, and 24 months was used.

Glucose tolerance test

To assess the metabolic response to glucose, a GTT was performed in TLR4 inhibitor treated mice as well as in young and old $Tlr4^{fl/LyzM\text{-}cre}$ and their respective controls. One week before sacrifice, mice were fasted for 6 hours. Body weight (BW) and fasting blood glucose were measured from blood collected via the lateral tail vein. Subsequently, glucose (2 g/kg BW, 20 % glucose solution) was injected intraperitoneally (i.p.), and blood glucose levels were measured from the lateral tail vein at 15, 30, 60, 90, and 120 minutes post-injection. The area under the curve was calculated in GraphPad Prism (Version 10.5.0) and adjusted to each animal's baseline fasting glucose levels.

Isolation of Langerhans islets

Langerhans islets were isolated from pancreatic tissue of young and old C57BL/6J mice as well as young and old WT and $Tlr4^{fl/LyzM\text{-}cre}$ mice following a previously described protocol with minor modifications [10, 25]. Directly after sacrifice, 3 ml of Liberase TL solution (Sigma-Aldrich, Germany) dissolved and diluted in HBSS (BIO&SELL, Germany) supplemented with 25 mM HEPES (Thermo Fisher Scientific, Germany) and 0.5 % bovine serum albumin (BSA) was injected into the common bile duct. Then the pancreas was digested in 2 ml Liberase TL solution at 37°C for 18 minutes. Following enzymatic digestion, the tissue was mechanically dissociated, and islets were separated from exocrine tissue using a Histopaque-Percoll gradient. Then the islets were hand-picked under a stereomicroscope. Depending on downstream application, they were either washed three times with phosphate-buffered saline (PBS) for gene expression analysis or incubated in $RPMI^{+}$ media (BIO&SELL, Germany, 2g/l glucose (11.1 mM), supplemented with L-glutamine, penicillin/Streptomycin, and 10% fetal bovine serum) at 37° C for functional assays.

Glucose-stimulated insulin secretion

To measure glucose-stimulated insulin secretion (GSIS) from young and old $Tlr4^{fl/LyzM\text{-}cre}$ mice and their respective controls, 40 islets per animal were recovered overnight after isolation in $RPMI^{+}$ medium at 37°C, 5% CO_2. The next day, islets were washed in Krebs-Ringer-bicarbonate HEPES buffer (KRBH) containing 0.1 % BSA. Subsequently, 15 islets (in duplicates) per animal were equilibrated for 1h in KRBH + BSA (without glucose) and then stimulated with different glucose concentration as previously described [10, 25]. Briefly, basal insulin secretion was assessed by low glucose stimulation (1 mM glucose), followed by high glucose stimulation (25 mM glucose) and finally depolarization with 40 mM potassium chloride in the presence of 1 mM glucose. Supernatants were collected for insulin measurement and normalized to the DNA content of islets.

DNA measurement of Langerhans islets

For normalization of insulin secretion to cellular DNA content, islets used in the GSIS assay were lysed and sonicated. DNA was quantified using the PicoGreen dsDNA Assay (Thermo Fisher Scientific, Germany) according to the manufacturer's instructions. Fluorescence measurement at excitation wavelength of 450 nm and emission wavelength of 520 nm was performed and the DNA content of the islets calculated by a standard curve.

Determination of plasma insulin and pancreatic islet secreted insulin

According to manufacturer's manual an Ultrasensitive Mouse Insulin ELISA (ALPCO, USA) was used to determine insulin concentration in plasma samples and supernatants of Langerhans islets.

Staining of isolated, dispersed Langerhans islets

Isolated Langerhans islets were enzymatically dispersed to single cells by incubation with Accutase (Pan Biotech, Germany) for 18 min at room temperature (RT), followed by washing with PBS. After fixation with 4% formaldehyde at RT for 10 min, cells were washed and

blocked with 10 % normal goat serum in DAKO antibody diluent (Agilent, Germany). Primary antibodies against TLR4 (anti-mouse, 1:50, ab22048, Abcam, United Kingdom) and insulin (anti-rabbit, 1:1000, ab181547, Abcam, United Kingdom) were applied in DAKO antibody diluent (Agilent, Germany) and incubated for one hour at RT. This was followed by washing steps and secondary antibody incubation (anti-mouse Alexa Fluor 594, A-11032, anti-rabbit Alexa Fluor 488, A-11008, Invitrogen, USA). Stained cells were mounted in Fluoromount-G with DAPI (Carl Roth, Germany) in glass-bottom dishes. Imaging was performed on a Zeiss LSM 780 confocal microscope (Zeiss, Germany) with a 20x, 0.8 objective using four different z-stack levels, and maximum intensity projections were generated for representative images.

In vitro culture of Langerhans islets and stimulation

After isolation, islets from old mice were pooled and incubated overnight in RPMI+ media ((BIO&SELL, Germany), containing 2g/l glucose, supplemented with L-glutamine, penicillin/streptomycin, and 10% fetal bovine serum). On the following day, islets were transferred into a 24-well plate (n = 3 biological replicates, 160 – 200 islets per condition, three conditions). A control group receiving vehicle, a group stimulated with 1 µg/ml LPS (*Escherichia coli* O55:B5, Sigma Aldrich, Germany) dissolved in 0.9% NaCl (1 mg/ml stock solution, diluted 1:1000) (Sigma Aldrich), and a group treated with 10 µM TAK-242 (Sigma Aldrich, Germany) dissolved in DMSO (10mM stock solution, diluted 1:1000) prior to 1 µg/ml LPS stimulation. All conditions contained equivalent amounts of DMSO (0.1%) and 0.9% NaCl as vehicle. For pre-treatment, TAK-242 or vehicle was applied 2 hours, followed by 6 hours of stimulation with LPS or NaCl, respectively. After stimulation islets were hand-picked again, washed three times with PBS and snap-frozen for subsequent mRNA isolation and gene expression analysis.

mRNA Isolation and quantitative real-time polymerase chain reaction (qPCR)

Total mRNA was isolated from islets using the Dynabeads™ mRNA DIRECT™ Kit (Invitrogen, USA) according to the manufacturer's instructions and eluted in 15 µl Tris-HCl buffer at 70°C and subsequent synthesized to cDNA. Therefore, the GoScript™ Reverse Transcriptase (Promega, Germany) was used according to the manufacturer. cDNA was then diluted 1:5 or 1:10 with nuclease free water. The qPCR analysis was performed using a MasterMix containing 1 µl DreamTaq™ buffer, 0.05 µl DreamTaq™ Hot Start DNA-Polymerase (Thermo Fisher Scientific, Germany), 2 mM dNTPs (Bioline, United Kingdom), 1x SYBR™ Green (Sigma Aldrich, Germany), 1.25 µM forward and reverse primers (*tumor necrosis factor alpha (TNFα), insulin 2 (Ins2), β-Actin*, r*ibosomal protein L13 a (RPL13a), hypoxanthine-guanine phosphoribosyl transferase (HPRT), myeloid differentiation primary response 88 (MyD88), interleukin 1 beta (IL-1ß), inducible nitric oxide synthase (iNOS), interleukin 6 (IL-6)*). All primers were obtained from Sigma Aldrich, Germany. The polymerase chain reaction started with a heating cycle of 3 min at 95 °C, followed by 40 cycles of denaturation for 15 s at 95 °C, primer hybridization for 30 s at 60°C – 65°C (primer dependent, Supplementary Table 1) and elongation for 30 s at 72°C. The Bio-Rad CFX Maestro 2.3 Software was used to calculate the relative gene expression using the ΔΔCt method normalized to the three housekeeping genes (*RPL13, HPRT,* β-*Actin*). Primer sequences are found in Supplementary Table 1. For gene expression of *CDKN2a/p16^{Ink4a}* a specific TaqMan® Gene Expression Assay (Mm00494449_m1, #4351370, Thermo Fisher Scientific, Germany,) was used. Reactions were performed according to the manufacturer's protocol with an annealing temperature of 60°C. Expression levels were normalized to the three housekeeper genes using the ΔΔCt method.

Immunohistochemical staining of paraffin embedded pancreatic sections

Paraffin embedded pancreatic sections (2 µm thickness) were prepared and stained immunohistochemically (IHC) with DAB-Chromogen (Agilent, Germany) as previously described [10]. Insulin was detected with anti-insulin antibody (1:40 000, ab181547, Abcam, United Kingdom) on two to three independent sectional planes and analyzed as described below. To identify macrophages within the pancreatic islets, anti-CD68 antibody (1:100, ab125212, Abcam, United Kingdom) was used.

Additional immunofluorescence staining in 2 µm sections was performed to identify further markers within insulin^{+} islets as previously described [10, 25, 26]. Briefly, paraffin embedded pancreatic sections were deparaffinized, antigen retrieval was performed (citrate buffer pH=6 or EDTA buffer pH=9) and, for intracellular located proteins, permeabilized (see **Table 1**). This was followed by 1 hour blocking at RT, primary antibody incubation overnight at 4°C and secondary antibody incubation including DAPI (1 hour at RT). Primary antibodies and staining conditions are listed in **Table 1**. Alexa-Fluor conjugated antibodies (anti-mouse 488 A-11029, anti-mouse 633 A-21052, anti-rabbit 633 A-21071, anti-rabbit 488 A-11008, anti-rat 546 A-11081, anti-rat 633 A-21094, Invitrogen, USA) were used and all

sections were counterstained with DAPI and mounted for imaging. Immune cell accumulation was assessed by staining for CD45, CD3, and CD8a to detect leukocytes and T-cell subsets within and around the islets (peri-insulitis). Proliferative potential in islet cells was assessed via proliferating cell nuclear antigen (PCNA) staining. Fibrotic remodeling and activated pancreatic stellate cells were visualized using α-smooth muscle actin (αSMA) staining. To assess the islet composition, tissue sections were stained with insulin (β-cells), glucagon (α-cells) and somatostatin (δ). All primary antibodies used are well established and were validated using secondary antibody-only and isotype controls (rabbit IgG isotype control #02-6102, mouse IgG isotype control #02-6502, rat IgG isotype control #02-9602, Invitrogen, USA). Unspecific staining artifacts in pancreatic tissue were mainly observed in blood vessels and did not affect the analyses.

Table 1. Immunofluorescence staining list.

Primary Antibody dilution	Company	Antigen Retrieval	Permeabilization [0,2 % Triton-X-100]
Insulin 1:1000 **CD45 1:50**	Abcam (ab181547) Bioscience (#559864)	Citrat pH =6	No
Insulin 1:1000 **PCNA 1:1000**	Abcam (ab181547) Cell Signaling (#2586)	Citrat pH =6	Yes
Insulin 1:200 **αSMA 1:500**	Cell Signaling (#8138) Cell Signaling (#19245)	Citrat pH =6	Yes
CD3 1:50 **CD8a 1:50**	Abcam (ab11089) Abcam (ab217344)	EDTA pH = 9	No
Glucagon 1:200 **Somatostatin 1:200** **Insulin 1:100**	Abcam (ab10988) Abcam (ab111912) Novus Bios (MAB1417)	Citrat pH =6	Yes

Image analysis and β-cell mass quantification

All stained sections were scanned either with the MIRAX Scanner or AxioScan Z.1/ AxioScan 7 (Zeiss) using a 5x magnitude for the coarse focus and a 20x, 0.8 objective for the fine focus. Image analysis was performed in Zen version 2.6/3.5. For immune cell subtype accumulation within and around the islet, $CD45^+$, $CD68^+$, $CD3^+$ and $CD8a^+$ cells were counted per islet. For the analysis of the proliferation potential, $PCNA^+$ nuclei in the islet were analyzed, using a threshold based automatic analysis. First, the islet region was identified via $insulin^+$ staining, followed by a subclass marking all nuclei ($DAPI^+$), and subsequently $PCNA^+$ nuclei. The mean ratio of $PCNA^+$ nuclei/ total islet nuclei of approximately 15 islets per animal was calculated. For the quantification of αSMA, the $Insulin^+$ area followed by the $αSMA^+$ area within islets ($insulin^+$) were determined via automatic image analysis in Zen or ImageJ by setting thresholds for the different fluorescent channels. For the islet composition threshold-based analysis of glucagon, insulin and somatostatin positive area was performed and ratios to total islet area calculated. For the calculation of the β-cell mass per animal, insulin was stained in three sectional planes and the area threshold based quantified. Then the ratio of $Insulin^+$ area to total pancreas area was averaged from the three sections and multiplied by the pancreas weight (β-cell mass = ($Insulin^+$ area/total pancreas area) * pancreas weight).

Histopathological scoring of insulitis and fibrosis

To determine age-related pancreatic tissue degeneration, two established scoring systems, one for immune cell infiltration (insulitis) and one for fibrosis, were applied. Insulitis scoring was based on insulin-positive islets identified by immunohistochemical staining. Infiltration of immune cells into and around pancreatic islets was assessed according to previously published criteria [10, 27-30]. Additionally, all pancreatic tissue samples were scored in two to three sectional planes and scoring was performed independently and blinded by two investigators.

For fibrosis, fibrotic structures were visualized by staining collagen fibers using Masson's Trichrome. A previous published fibrosis score was used that distinguishes five different stages of fibrosis [10]. For each animal sample, 20-30 islets were scored by two blinded investigators.

Measurement of TLR4 ligands in pancreatic tissue and endotoxin in mouse plasma

To determine the presence of TLR4 ligands, a commercially available SEAP-reporter assay using transfected HEK293 cells (Invivogen, USA) was used as detailed before. Briefly, snap-frozen pancreatic tissue was homogenized in pyrogen-free water, sonicated for 1 min and supernatant was applied to the reporter cells as

previously described [31]. Data was presented normalized to total protein content of each sample. For the detection of plasma endotoxin levels in young and old mice, the Limulus amoebocyte lysate assay (Charles River, France) was used according to the manufacturer's instructions with adaptions as previously described [32].

Glycogen measurement in quadriceps muscle tissue

Snap-frozen quadriceps tissue from young and old $Tlr4^{fl/LyzM\text{-}cre}$ mice and their respective WT was grounded under liquid nitrogen. After extraction in 0.1 mol/L sodium hydroxide, glycogen concentrations were determined (Starch Kit, R-Biopharm, Germany) and normalized to protein content (DC Protein Assay Reagents, Bio-Rad, USA).

Statistical analysis

All statistical analyses were performed with GraphPad Prism Version 10.5.0. For group sizes $n>3$ Outlier test based on Grubb's was conducted. After testing for normalization, two groups were compared using unpaired Student's *t*-test or Mann-Whitney *U* test for non-parametrically distributed values. For comparison between three groups, an ordinary one-way ANOVA depending on data distribution (Tukey's-, Dunn's-, Šídák's - or Holm-Šídák's multiple comparisons test) was performed. For grouped analysis a two-way ANOVA with multiple comparisons and uncorrected Fisher's LSD was performed. All values are presented as mean +/- standard deviation (SD) unless otherwise stated. For ordinal data (insulitis and fibrosis scores) only the mean value is reported. Results with a p value < 0.05 were considered as statistically significant.

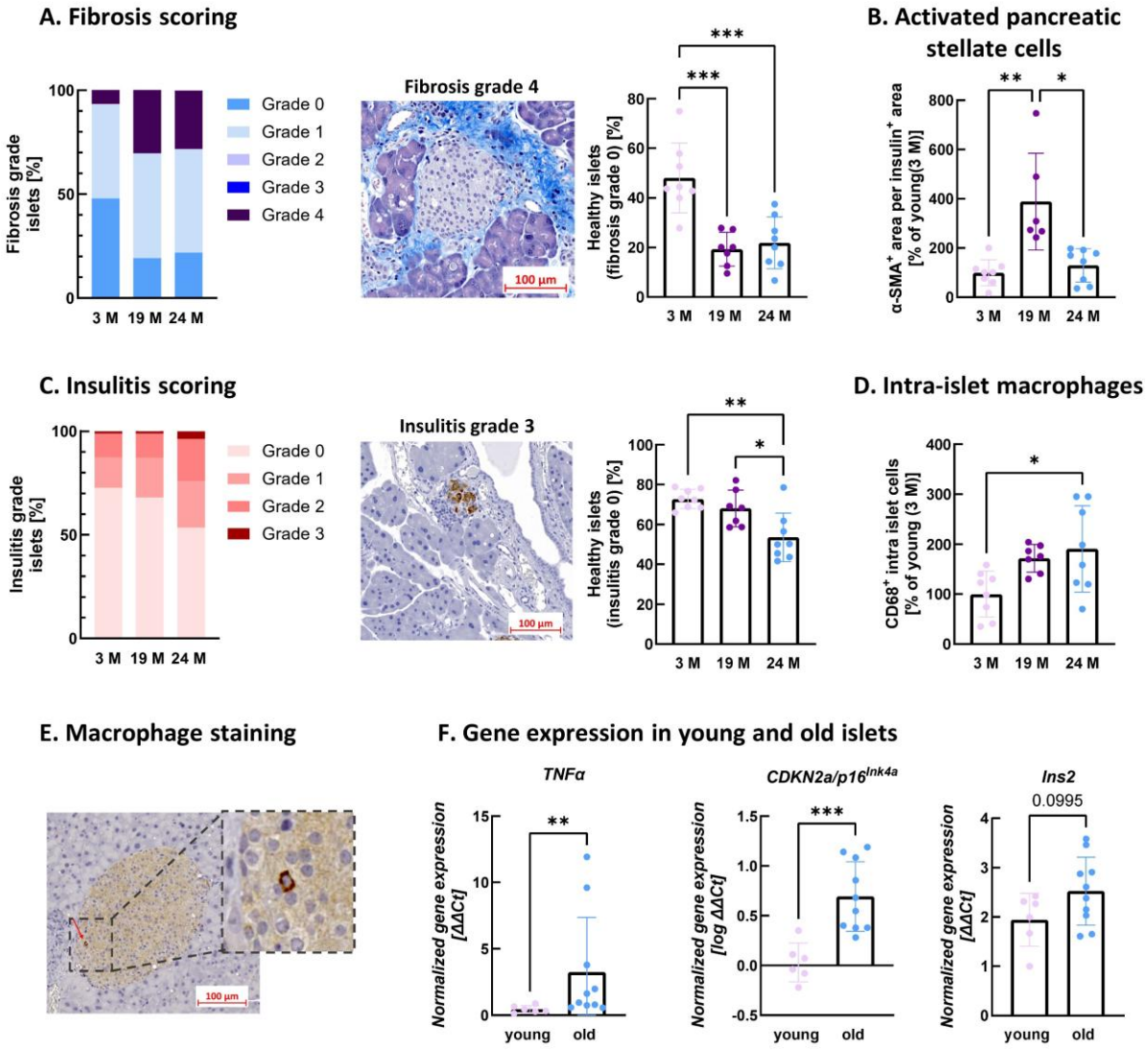

Figure 1. Age-related structural and inflammatory changes in pancreatic islets. (A) Fibrosis of Langerhans islets, representative image (20x magnification) of a fibrotic islet and healthy islets (grade 0 fibrosis) in male C57BL/6J mice; n=7-8. **(B)** Activation of pancreatic stellate cells by αSMA-staining in Langerhans islets in male C57BL/6J mice; n= 7-8. **(C)** Insulitis, representative image of an insulitis islet and healthy islets (grade 0 insulitis) in male C57BL/6J mice; n=7-8. **(D)** Intra-islet macrophages ($CD68^+$cells) in male C57BL/6J mice; n=7-9. **(E)** Representative image of macrophage ($CD68^+$) staining in pancreatic tissue. **(F)** Gene expression results of young (3 months) and old (26 months) male and female mice in Langerhans islets for *TNFα, CDKN2a/p16* ^{Ink4a} and *Ins2;* n= 6-10. Data are presented as mean +/- SD or mean; depending on normality, statistical analysis by unpaired Student's *t*-test or Mann-Whitney *U* test for comparison between two groups or ordinary one-way ANOVA (Tukey's multiple comparison test or Dunn's multiple comparison test) for comparison between 3 groups. * p<0.05; ** p<0.01; *** p<0.001. Ins2= Insulin 2, SD= standard deviation; TNFα= tumor necrosis factor α.

RESULTS

Aging increases inflammation and fibrosis in old islets

We have previously demonstrated that aging in mice is associated with increased fibrosis and insulitis in pancreatic islets [10]. To further support this dataset, we analyzed now distinct aging stages in pancreatic tissue sections from mice aged 3, 19, and 24 months. The current dataset supports and extends previous findings by confirming both pathological features in independent cohorts covering distinct aging stages. In particular, the proportion of fibrotic islets, identified by morphology and αSMA staining, was significantly increased in 19-month-old animals, with no further increase observed at 24 months, suggesting a plateau in fibrotic remodeling (Fig. 1A, B). In contrast, insulitis prevalence and the number of macrophages ($CD68^+$ cells) were most pronounced at 24 months, indicating a late-onset inflammatory response in pancreatic islets (Fig. 1C-E). In addition, analysis of intrapancreatic adipocyte infiltration, considered a potential contributor to inflammation, revealed greater variability in aged animals, but no significant increase was observed (see Supplementary Fig. 3A). To support the histological observations, gene expression analysis was performed in isolated islets from young (5 months) and old (26 months) mice, showing an increased expression of the cytokine *TNF-α* as well as higher expression of the senescence marker *CDKN2a/p16*^{Ink4a}, while *Ins2* expression tended to decline in aged islets (Fig. 1F).

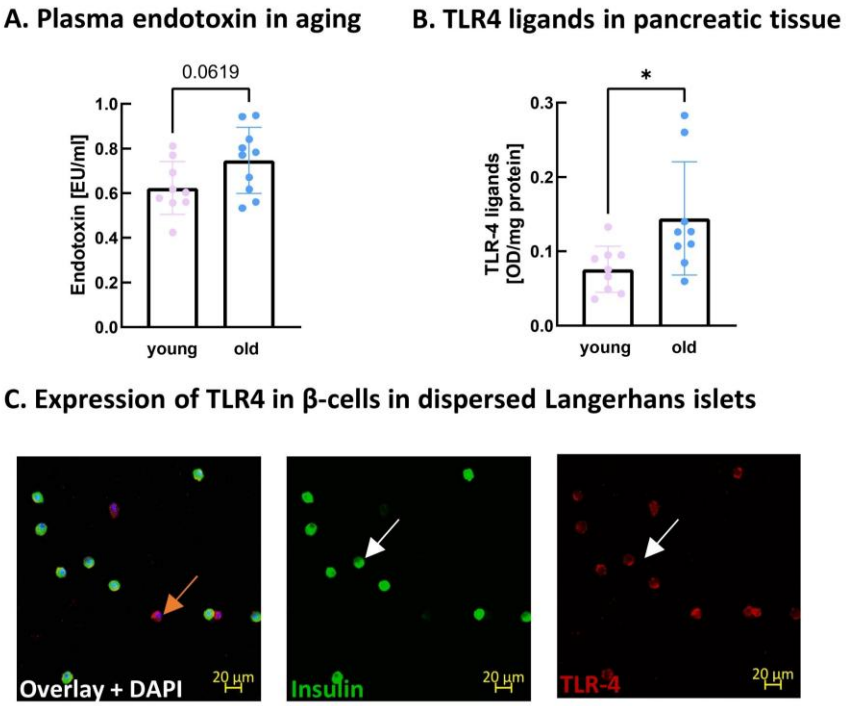

Figure 2. Increased TLR4 ligands with age and cellular localization in islets. (**A)** Measurement of endotoxin in plasma from young and old male C57BL/6J mice; n= 9-10, mean +/- SD, unpaired Student's *t*-test. (**B)** Measurement of TLR4 ligands in pancreatic tissue lysate from young and old C57BL/6J mice via SEAP-reporter assay; n= 10, mean +/- SD, Mann-Whitney *U* Test, *p<0.05. (**C)** Representative image of TLR4 and Insulin co-staining in dispersed murine Langerhans islets from old C57BL/6J mice; orange arrow pointing at non-insulin, presumably immune cells while white arrows are showing TLR4 expression in insulin-positive accordingly β-cells. SD = standard deviation, TLR4 = Toll-like receptor 4.

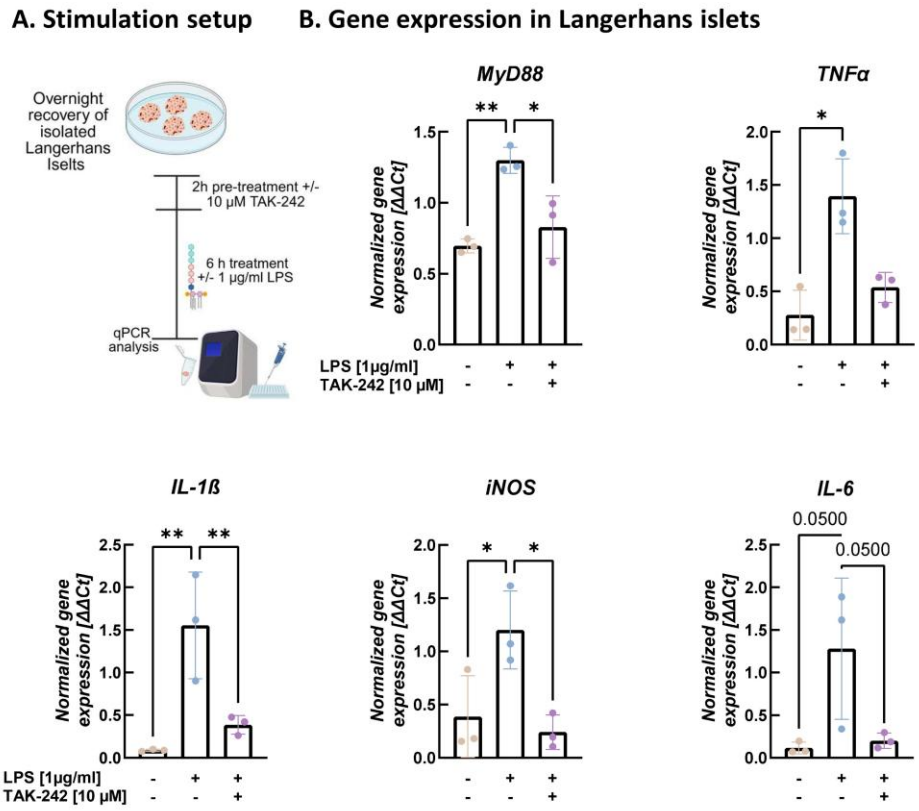

Figure 3. ***Ex vivo*** **LPS stimulation of aged islets with and without TLR4 inhibition. (A)** Experimental setup for the stimulation of Langerhans islet, Created in BioRender. Jelleschitz, J. (2025) https://BioRender.com/eb3k0lk. **(B)** Gene expression in Langerhans islets of *MyD88*, *TNFα*, *IL-1β*, *iNOS* and *IL-6*. Data are mean +/- SD, n=3, ordinary one-way ANOVA between selective groups (Šídák's multiple comparisons test or Holm-Šídák's multiple comparisons test); *p<0.05, **p<0.01. IL = Interleukin, iNOS = inducible nitric oxide synthase, LPS = Lipopolysaccharide, SD = standard deviation, MyD88 = myeloid differentiation primary response 88, TNFα = tumor necrosis factor α.

Age-related increase of TLR4 ligands and β-cell TLR4 expression

Bacterial toxins are known inducers of inflammation and may increase during aging, possibly due to increased intestinal permeability [33, 34]. Measurement of plasma endotoxin concentration in young and old mice revealed a trend (p = 0.0619) towards higher levels in aged mice (Fig. 2A). To assess whether such inflammatory stimuli might directly affect the pancreas, TLR4 ligands were quantified in pancreatic tissue lysates and were significantly elevated in aged mice compared to young controls (Fig. 2B). Furthermore, single-cell immunofluorescence staining of dissociated murine Langerhans islets demonstrated TLR4 expression in insulin-positive cells, suggesting that pancreatic β-cells may directly participate in TLR4 mediated signaling. However, TLR4 signal was also detected in insulin-negative cells, likely including immune cells, which are known to be the predominant site of TLR4 expression (Fig. 2C).

Effect of LPS stimulation and pre-treatment with TAK-242 on aged isolated Langerhans islets

Given that, in addition to intra-islet immune cells, β-cells also express TLR4, we examined whether ligand-mediated TLR4 activation and its pharmacological inhibition modulate islet inflammation. *Ex vivo* LPS stimulation did not reveal significant differences between young and old islets (Supplementary Fig. 2), possibly reflecting the absence of *in vivo* microenvironmental cues such as continuous cytokine exposure and immune-stromal interactions. We therefore focused on aged islets, which are characterized by higher basal immune cell infiltration and TLR4 expression.

Langerhans islets from old mice were isolated and recovered overnight, then pre-incubated with 10 µM TAK-242 or vehicle, followed by a 6 h stimulation with 1 µg/ ml LPS (Fig. 3A). Gene expression analysis revealed an LPS-dependent increase in TLR-signaling pathways indicated by higher *MyD88* expression and elevated levels of pro-inflammatory markers (*TNFα, IL-1β, iNOS, IL-6*)

compared to the untreated control. In addition, pre-treatment with TAK-242 inhibited LPS-induced increase of *MyD88* and cytokine and *iNOS* expression, reducing the LPS-dependent inflammatory signal (Fig. 3B).

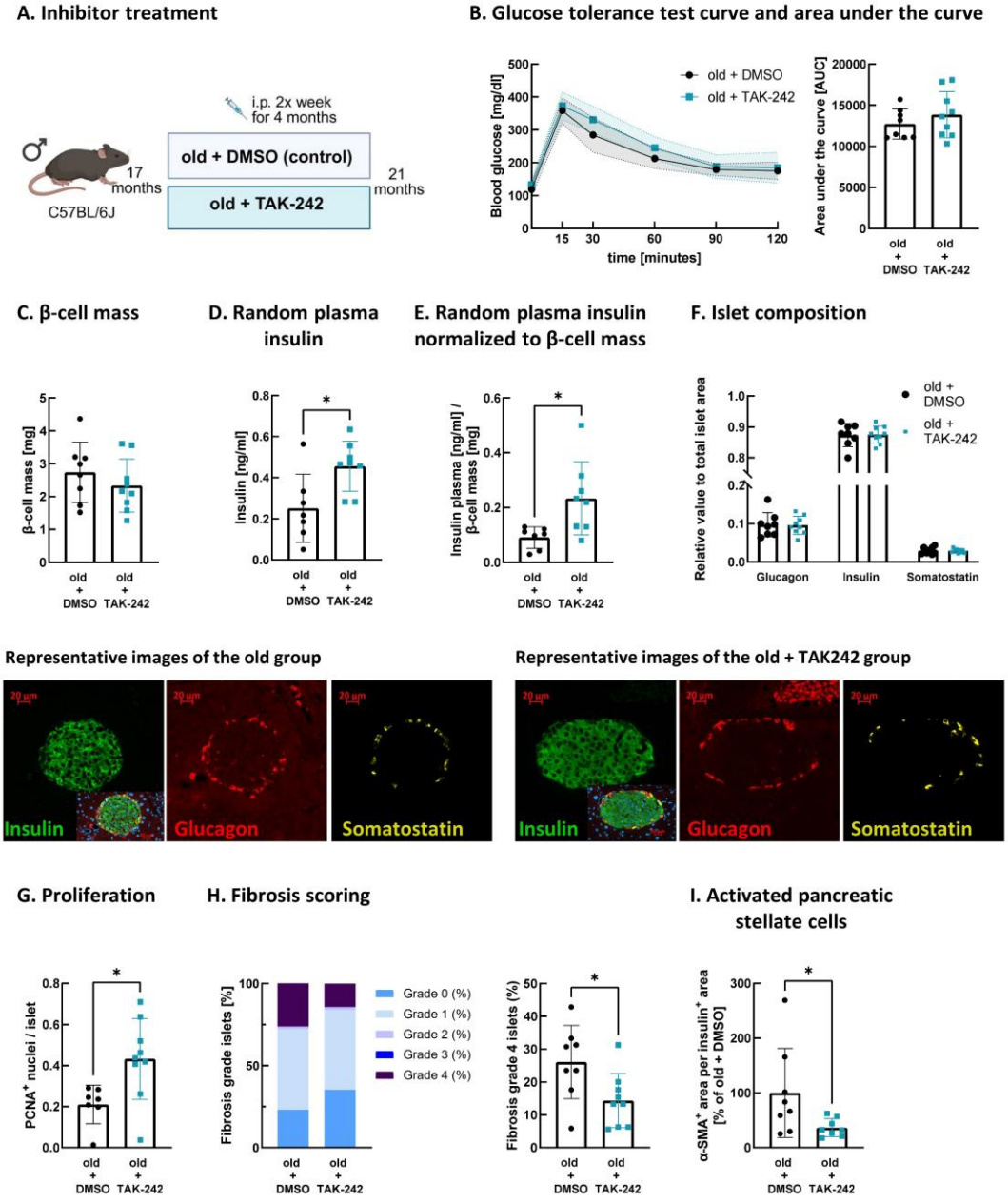

Figure 4. Pharmacological TLR4 inhibition ameliorates age-related islet alterations. (A) Study design of inhibitor treatment in aged, male C57BL/6J mice. Created in BioRender. Jelleschitz, J. (2025) https://BioRender.com/eb3k0lk. **(B)** Glucose tolerance and area under the curve. **(C)** β-cell mass of pancreatic tissue. **(D)** Random plasma insulin. **(E)** Random plasma insulin normalized to β-cell mass. **(F)** Islet Composition of α-, β- and δ-cells with representative immunofluorescence panel for the staining of old mice and old+TAK242 mice, showing α-cells (glucagon positive), β- cells (insulin positive) and δ-cells (somatostatin positive). **(G)** Proliferative nuclei in Langerhans islets. (H) Fibrosis Scoring and Grade 4 fibrotic islets. **(I)** αSMA staining to analyse activated pancreatic stellate cells. All data are mean +/- SD or mean; n= 8-9; Unpaired Student's t-test or Mann-Whitney U test; *p<0.05. DMSO = dimethyl sulfoxide, i.p. = intraperitoneal, PCNA=proliferating cell nuclear antigen, SD = standard deviation.

TAK-242 treatment influences insulin secretion and reduces fibrosis of Langerhans islets

To assess whether TLR4 inhibition can modulate age-related structural, functional, and inflammatory changes in Langerhans islets *in vivo*, 17-month-old C57BL/6J mice, an age at which circulating TLR4 ligand levels are elevated [33], were treated with TAK-242 or vehicle for four months (Fig. 4A). No difference in body weight and weight gain were observed between the groups (Supplementary Table 2). Glucose metabolism was assessed by an intraperitoneal glucose tolerance test (GTT) prior to sacrifice. However, the response to glucose did not differ between both groups as shown by the calculation of the area under the curve (Fig. 4B). As β-cell mass may increase with age and might be an early first sign of β-cell compensation due to β-cell failure [35], embedded pancreatic tissue was stained for insulin. The calculated β-cell mass was not affected by TAK-242 treatment (Fig. 4C). However, random plasma insulin was increased in TAK-242 treated mice compared to untreated controls, and insulin secretion normalized to β-cell mass was likewise increased. This suggests that TLR4 inhibition may enhance the secretory capacity of β-cells without altering their overall mass (Fig. 4D, E). As aging may alter the relative proportions of α-, β-, and δ-cells within the islets and thereby influence β-cell function, pancreatic tissue was stained for these cell types and islet composition was quantified. However, no differences were observed between the groups (Fig. 4F).

To assess the proliferative potential of β-cells, nuclei positive for the proliferation marker PCNA were quantified within islets of both groups. The proportion of PCNA-positive nuclei within the islet was significantly higher in TAK-242 treated mice (Fig. G). Further histopathological characterization of the pancreatic tissue sections included fibrosis scoring of Langerhans islets. Indeed, TAK-242 treated mice showed a significantly higher proportion of grade 0 (healthy) islets and less grade 4 fibrotic islets (Fig. 4H). Consistently, αSMA positive staining within the islets was significantly reduced following TAK-242 treatment (Fig. 4I).

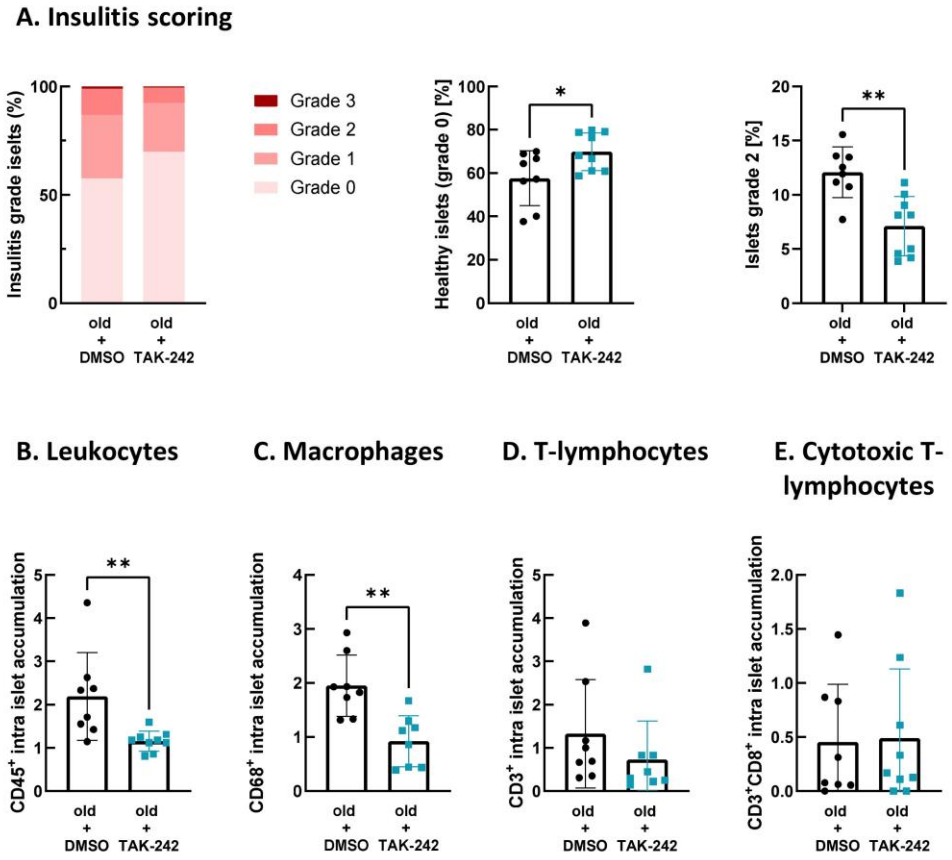

Figure 5. Reduced insulitis and immune cell infiltration by TLR4 inhibition in aged islets. (A) Insulitis Scoring, healthy islets and grade 2 islets. **(B)** Intra-islet leukocyte ($CD45^+$) accumulation. **(C)** Intra-islet macrophage ($CD68^+$) accumulation. **(D)** Intra-islet T-lymphocyte ($CD3^+$) accumulation. **(E)** Intra-islet cytotoxic T-lymphocyte ($CD3^+CD8a^+$) accumulation. All data are mean +/- SD or mean; n= 8-9; Unpaired Student's *t*-test or Mann-Whitney *U* test; *p<0.05. DMSO= dimethyl sulfoxide; SD = standard deviation.

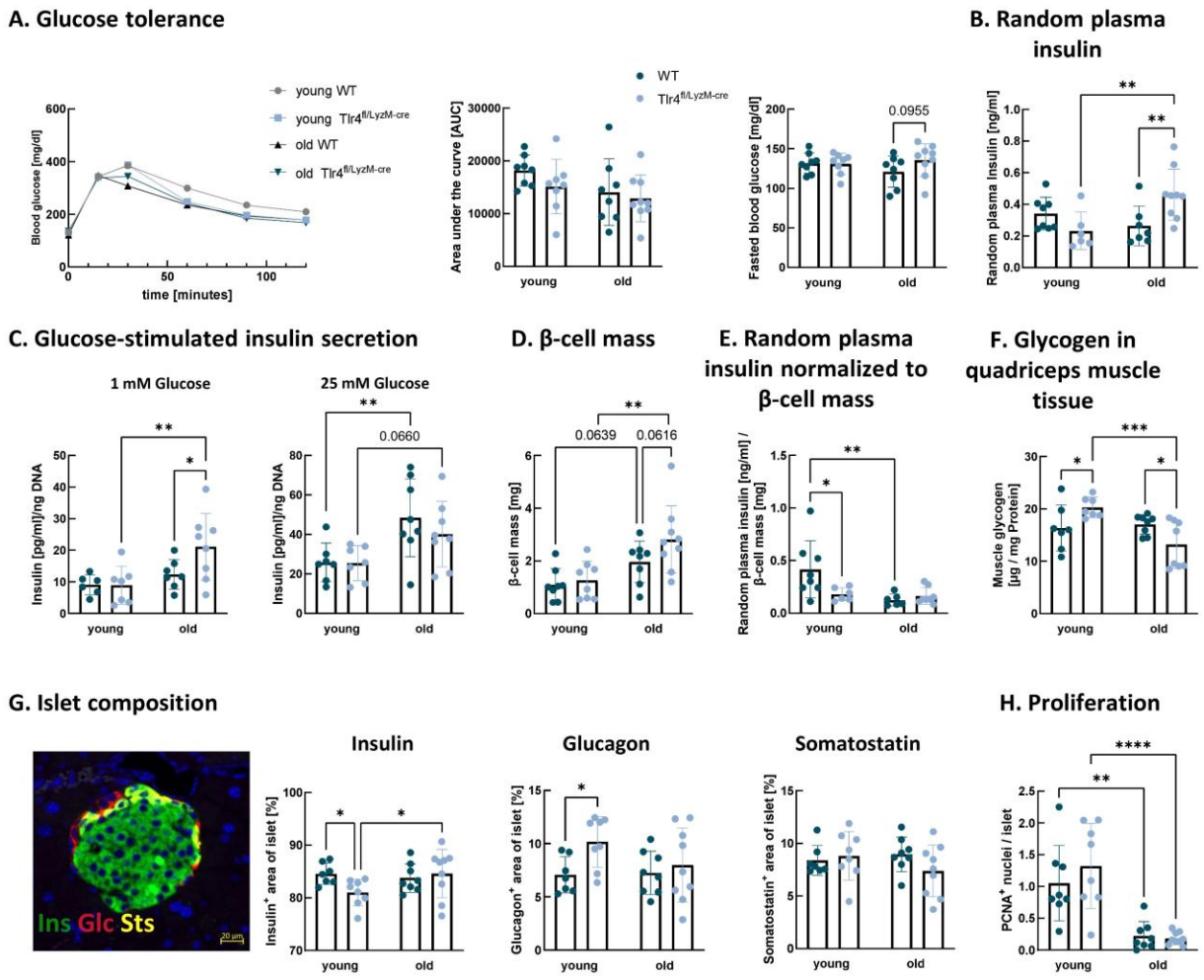

Figure 6. Myeloid-specific TLR4 deletion alters glucose metabolism and islet cell composition. (A) Glucose tolerance, area under the curve and fasting blood glucose levels in young and old $Tlr4^{fl/LyzM\text{-}cre}$ and WT mice. **(B)** Random plasma insulin. **(C)** Glucose-stimulated insulin secretion in isolated Langerhans islets under basal (1mM) and high (25 mM) glucose concentration. **(D)** β-cell mass in pancreatic tissue. **(E)** Random plasma insulin normalized to β-cell mass. **(F)** Glycogen measurement in quadriceps muscle tissue. **G.** Islet composition of α-, β-, and δ- cells. **(H)** Proliferative nuclei in Langerhans islets. All data are mean +/- SD or mean; n= 7-9; two-way ANOVA with uncorrected Fisher's LSD; *p<0.05, ** p<0.01; *** p<0.001; ****p<0.0001. SD = standard deviation, TLR4 =Toll-like receptor 4, WT= Wildtype.

Insulitis, and particularly macrophage accumulation in Langerhans islets is reduced by TAK-242 treatment in aged mice

A 4-month treatment in aged mice with TAK-242 attenuated the immune cell accumulation in islets compared to the untreated control. This was reflected by a significantly higher proportion of healthy islets, mainly due to a reduction in grade 2 infiltrated islets in the inhibitor-treated group (Fig. 5A). Consistently, while peri-insulitis accumulation of total leukocytes ($CD45^+$) remained unchanged, (Supplementary Fig. 1), a lower number of intra-islet leukocytes was observed (Fig. 5B). Analysis of immune cell subtypes revealed selectively reduced macrophage infiltration without affecting other immune cell populations due to the inhibitor treatment (Fig. 5C- E).

Myeloid-specific TLR4 deficiency may alter Langerhans islet composition and insulin secretion in aging

Since pharmacological TLR4 inhibition improved age-related changes in Langerhans islets by reducing insulitis, fibrosis, and macrophage infiltration, we next asked whether the absence of TLR4 in myeloid cells could represent a preventive scenario. To address this, a myeloid-specific TLR4 knockout model was used and young (4 months) and old (20 months) knockout and WT mice were examined to assess islet composition, β-cell function, and systemic glucose metabolism.

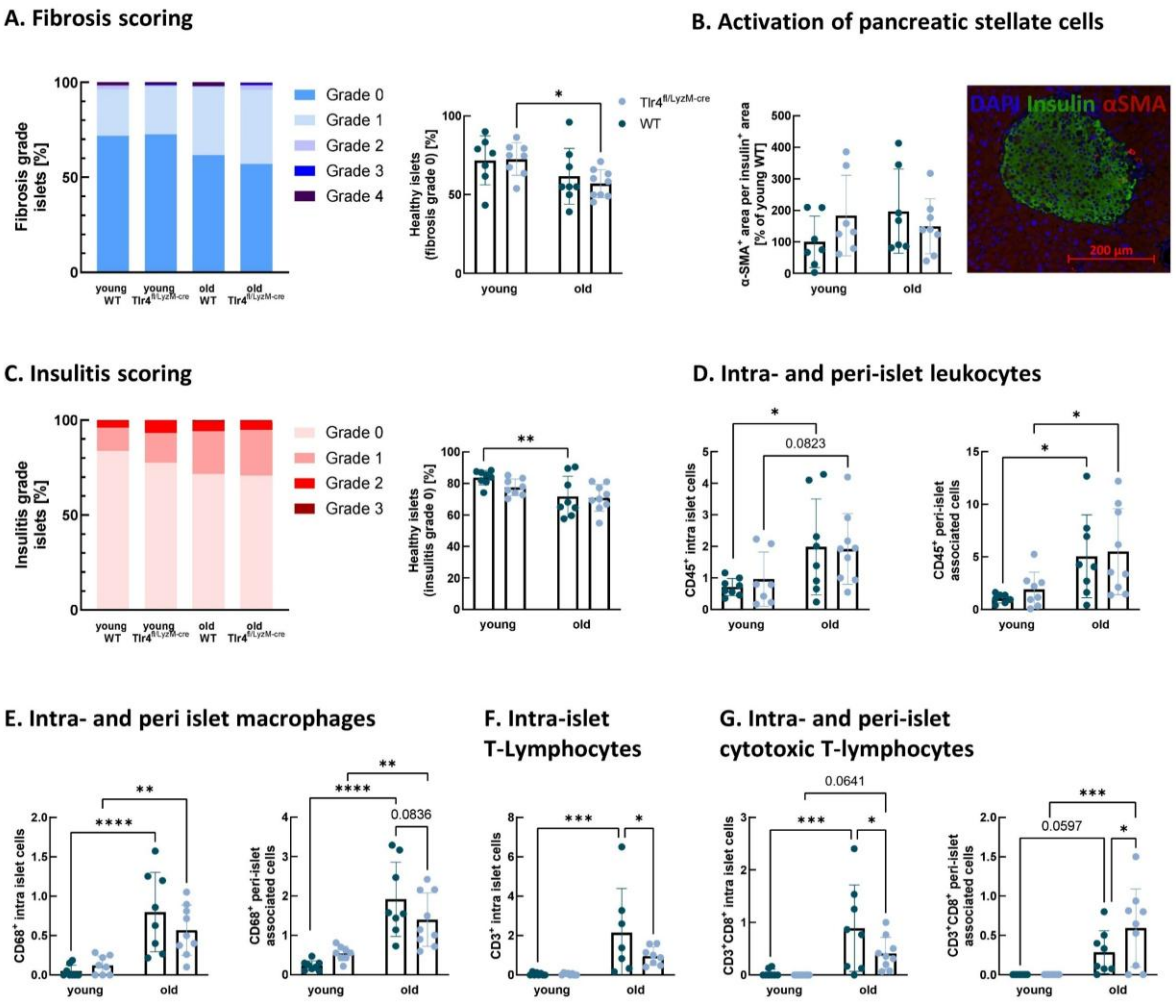

Figure 7. Impact of myeloid TLR4 deletion on islet fibrosis, insulitis, and immune infiltration. (A. Fibrosis scoring and healthy, non-fibrotic islets. **(B)** αSMA staining to analyse activated pancreatic stellate cells. **(C)** Insulitis scoring and healthy islets. **(D)** Intra- and peri-islet leukocytes ($CD45^+$). **(E)** Intra- and peri-islet macrophages**. (F)** Intra-islet T-lymphocytes. **(G)** Intra- and peri-islet cytotoxic T-lymphocytes. All data are mean +/- SD or mean; n= 8-9; two-way ANOVA with uncorrected Fisher's LSD; *p<0.05, ** p<0.01; *** p<0.001; ****p<0.0001. SD = standard deviation, TLR4 =Toll-like receptor 4, WT = Wildtype.

Glucose tolerance tests performed one week prior to sacrifice showed no significant differences in glucose clearance between groups, although aged $Tlr4^{fl/LyzM\text{-}cre}$ mice tended (p = 0.0955) to have higher fasting blood glucose than aged WT (Fig. 6A). Interestingly, random plasma insulin was higher in aged $Tlr4^{fl/LyzM\text{-}cre}$ compared with both young $Tlr4^{fl/LyzM\text{-}cre}$ and aged WT (Fig. 6B). In GSIS assays, islets from aged $Tlr4^{fl/LyzM\text{-}cre}$ mice secreted more insulin under basal glucose (1 mM) but showed a blunted response to high-glucose stimulation (25 mM) compared with aged WT mice (Fig. 6C). Besides that, also β-cell mass increased significantly in aged $Tlr4^{fl/LyzM\text{-}cre}$, and tends (p = 0.0626) to be higher than in aged WT mice. When random plasma insulin was normalized to β-cell mass, insulin output declined with age in WT mice, whereas this decline was already present in young $Tlr4^{fl/LyzM\text{-}cre}$ mice (Fig. 6E). Muscle glycogen levels were also affected by genotype and age: they were elevated in young $Tlr4^{fl/LyzM\text{-}cre}$ and declined with age, reaching levels significantly lower than those in aged WT mice (Fig. 6F). To asses, if the changed insulin secretion is linked to islet architecture, we performed triple staining for α-cells (glucagon positive), β-cells (insulin positive) and δ-cells (somatostatin positive). In young $Tlr4^{fl/LyzM\text{-}cre}$ mice, insulin-positive area was reduced, whereas glucagon-positive area was increased (Fig. 6G). Finally, proliferative activity was evaluated using PCNA staining and analysis revealed a significant age-related decrease of $PCNA^+$ nuclei within islets in $Tlr4^{fl/LyzM\text{-}cre}$ as well as in WT, indicating reduced proliferative capacity with aging regardless of genotype (Fig. 6H).

Myeloid TLR4 deficiency alters immune cell composition without affecting islet fibrosis or insulitis

Building on the observed alterations in islet function and cellular composition in $Tlr4^{fl/LyzM\text{-}cre}$ mice, the analysis was extended to determine whether myeloid-specific TLR4 deficiency affects structural remodeling and immune cell infiltration that characterize aging islets. In contrast to previous findings, we did not observe a significant decrease in healthy, non-fibrotic islets in aged WT mice. However, aged $Tlr4^{fl/LyzM\text{-}cre}$ showed a marked reduction compared to young $Tlr4^{fl/LyzM\text{-}cre}$ animals (Fig. 7A). Similarly, αSMA-positive area did not increase in WT controls of the current cohort, and αSMA staining remained unchanged across all groups, including aged $Tlr4^{fl/LyzM\text{-}cre}$ (Fig. 7B). Regarding insulitis, the proportion of non-infiltrated islets declined in aged WT mice, but not significantly in $Tlr4^{fl/LyzM\text{-}cre}$ mice (Fig. 7C). Despite this, intra-islet and peri-islet leukocyte accumulation increased in both genotypes (Fig. 7D), suggesting persistent immune cell activation in aging pancreas regardless of myeloid TLR4 signaling. Subtype-specific analysis revealed that macrophages ($CD68^+$) were elevated in both aged groups, although peri-islet macrophage accumulation tended to be lower in aged $Tlr4^{fl/LyzM\text{-}cre}$ ($p = 0.0836$; Fig. 7E). T-lymphocytes ($CD3^+$) were significantly elevated only in old WT mice (Fig. 7F). Despite that, further characterization of T-lymphocytes revealed an increase in intra-islet cytotoxic T-cells ($CD3^+CD8a^+$) in both aged genotypes, but significantly lower in the old $Tlr4^{fl/LyzM\text{-}cre}$ mice compared to the old WT mice. In contrast, peri-islet accumulation of cytotoxic T-cells revealed a significant increase in old $Tlr4^{fl/LyzM\text{-}cre}$ compared to their young counterparts and even exceeded levels observed in aged WT mice (Fig. 7G). Overall, these findings suggest that while myeloid-specific TLR4 deletion does not attenuate fibrotic or inflammatory islet remodeling during aging, it alters the subtype composition and spatial distribution of immune cells within the islet microenvironment.

DISCUSSION

A progressive decline in β-cell function in aging contributes to the increased prevalence of T2D in the elderly [36, 37]. Among lifestyle factors and genetic predisposition, the role of chronic, low-grade inflammation partly driven by a higher intestinal permeability and increased bacterial toxins, in particular LPS, is increasingly recognized as contributor [38-40]. This inflammatory milieu can also precede overt T2D and directly impair β-cell function [41, 42]. In fact, in our aging cohort, plasma endotoxin levels tended to be higher in old mice, and pancreatic TLR4 ligands were significantly elevated (Fig. 2A, B). Single-cell immunostaining (Fig. 2C) confirmed TLR4 expression not only in immune, but also in insulin-positive cells, indicating that both resident immune cells and β-cells may directly respond to bacterial ligands and contribute there to local inflammation. These changes coincided with increased insulitis, macrophage infiltration, fibrosis, elevated *TNFα*, and induction of the senescence marker *CDKN2a/p16*^{Ink4a}, suggesting that TLR4-mediated inflammation is a plausible driver of age-related islet dysfunction (Fig. 1). Interestingly, while fibrotic and immune cell accumulation were clearly pronounced in aging tissue, adipocyte depots, which are also known to promote inflammation [43], were not significantly elevated in aging pancreatic tissue. Also blocking TLR4 resulted in no change of adipocyte depots (Supplementary Fig. 3). Locally increased inflammation in aged islets may impair β-cell function potentially by changing insulin gene expression. In line with this, Maedler et al. demonstrated, that TLR4 activation by LPS can impair β-cell function and accordingly insulin secretion, via induction of cytokine and chemokine expression [38, 44]. Therefore, targeting TLR4 to block downstream cytokine induction could reduce local islet inflammation and preserve β-cell function during aging.

To determine whether pharmacological inhibition of this pathway could mitigate age-associated islet dysfunction and remodeling, aged mice were treated for four months with the selective TLR4 inhibitor TAK-242. TAK-242 disrupts the interaction of TLR4 with adaptor molecules by binding to the Cys747 residue in its intracellular domain [45, 46]. In previous studies, administration of TAK-242 in muscle tissue could prevent insulin resistance [47, 48], which is closely linked to proper β-cell function. However, its inhibitory effect in Langerhans islets remains largely unexplored. *In vitro* experiments in human Langerhans islets from Maedler et al. [38], as well as our studies in murine islets (Fig. 3), demonstrated that the inhibitor can directly suppress LPS-induced cytokine expression in Langerhans islets by inhibiting the activation of *MyD88* gene expression. After confirming this short-term inflammatory effect *ex vivo*, we performed *in vivo* experiments in aged animals, at a stage when circulating bacterial toxins are known to be elevated as seen in previous experiments [33]. From this time point, male C57BL/6J mice received a four-month treatment with TAK-242 or DMSO as vehicle (Fig. 4A). Fibrosis, one of the earliest signs of tissue aging, was reduced in islets from TAK-242–treated animals. This effect is likely mediated by successful reduction of TLR4/MyD88/NF-κB signaling, consistent with findings from Liu et al. in liver tissue [49]. Further, in preclinical fibrosis models TAK-242 attenuated fibrosis by reducing the production of pro-fibrotic mediators and accordingly

attenuated collagen synthesis and myofibroblast differentiation [50]. In line with this mechanism, we observed, that the inhibitor treatment reduced αSMA$^+$ staining in islets (Fig. 4I). This is marker for activated pancreatic stellate cells (PSC), which, upon cytokine stimulation, transform into collagen-producing myofibroblasts that drive islet fibrosis. [51, 52]. Although β-cells are generally considered postmitotic with only minimal proliferation capacity in aging [26, 53], TAK-242 treatment partly preserved this potential, as evidenced by an increased number of PCNA$^+$ nuclei in islets (Fig. 4G). Combined with the observed increase in random plasma insulin, even when normalized to β-cell mass (Fig. 4D, E) and remaining below hyperinsulinemic levels, these findings support the maintenance of β-cell function in aging.

Despite these local improvements, including reduced insulitis, fibrosis, and preserved β-cell proliferative potential, these effects did not translate into systemic metabolic benefits (Fig. 4B), possibly due to the relatively short intervention period. Moreover, circulating insulin reflects both β-cell secretion and systemic clearance, including enzymatic degradation by insulin-degrading enzyme ([54-56]. As insulin clearance was not assessed, interpretations of β-cell function from plasma insulin levels remain limited. Additionally, heterogeneity in insulin sensitivity among aged C57BL/6J mice [57] may further obscure links between local islet improvements and systemic glucose control. Nevertheless, clear histological improvements were observed, also regarding immune cell infiltration frequently accompanying fibrotic changes, as evident in our aging cohort (Fig. 1).

Insulitis, originally described in diabetic conditions [58-60], was recently demonstrated by us in healthy aging mice [10], showing immune cell profiles similar to diabetic phenotypes. Treatment with TAK-242 reduced immune cell accumulation, especially islets scored grade 2 (<50% immune cell infiltration). This reduction was driven by fewer intra-islet leukocytes (CD45$^+$), whereas peri-islet leukocytes remained unchanged (Fig. 5, Supplementary Fig. 1). Subtype analysis revealed a selective decrease in macrophage accumulation (CD68$^+$) but not in T-lymphocytes. Given that macrophages are among the first immune cells to initiate insulitis, increase in autoimmune diabetes before T-cell involvement [61, 62], and express high levels of TLR-4, they are likely the primary mediators of the observed inhibitor effect [63]. These findings suggested a potentially critical role of myeloid TLR4 signaling in age-related islet inflammation and β-cell decline, which was further addressed using a myeloid-specific TLR4 knockout model.

Contrary to the initial hypothesis, which predicted that myeloid-specific TLR4 deletion would attenuate inflammation and improve age-related β-cell dysfunction, old Tlr4$^{fl/LyzM\text{-}cre}$ mice instead showed disturbed glucose homeostasis and altered insulin dynamics compared to age-matched WT controls. While glucose tolerance was unaffected, fasting blood glucose tended to be elevated, and GSIS assays revealed increased basal insulin secretion in old Tlr4$^{fl/LyzM\text{-}cre}$ islets (Fig. 6 A, C) - a feature commonly associated with early insulin resistance and type 2 diabetes [64]. Further, random plasma insulin was solely elevated in aged Tlr4$^{fl/LyzM\text{-}cre}$, but when normalized to β-cell mass, insulin output was already reduced in young Tlr4$^{fl/LyzM\text{-}cre}$ mice, suggesting an early defect in β-cell secretory capacity (Fig. 6B, E). Additionally, β-cell mass was markedly increased in aged Tlr4$^{fl/LyzM\text{-}cre}$ mice, and together with age-associated reduced proliferation potential of β-cells shown by reduced PCNA$^+$ nuclei (Fig. 6D, G), resembles compensatory β-cell hypertrophy seen in diabetic models. Impaired insulin action was also observed in the quadriceps muscle tissue, as glycogen, initially elevated in young Tlr4$^{fl/LyzM\text{-}cre}$ mice, declined sharply with age in Tlr4$^{fl/LyzM\text{-}cre}$ mice (Fig. 6 F). Balanced immune cell signaling seems critical for β-cell function, since whole-body TLR4 knockout in non-obese mice used for autoimmune diabetes research even accelerated the diabetic phenotype by increasing β-cell mass, insulitis and insulin resistance [65]. In contrast, other studies showed an attenuation of the diabetic phenotype and β-cell dysfunction in TLR4 knockout models [66, 67], resulting in contradictory findings.

Interestingly, the lifelong absence of TLR4 signaling in myeloid cells may disrupt developmental priming of β-cell function. In young Tlr4$^{fl/LyzM\text{-}cre}$ mice, islet composition was altered, with reduced insulin-positive area alongside increased glucagon-positive area within pancreatic islets (Fig. 6G), pointing to an early imbalance in endocrine cell ratios. As macrophages are known to shape the islet microenvironment through cytokine production and tissue remodeling [68, 69], their inability to respond to TLR4 ligands could impair immune-endocrine crosstalk essential for β-cell maintenance and maturation. In contrast to the TLR4 inhibitor treatment, insulitis and fibrosis were neither attenuated nor accelerated by a myeloid-specific TLR4 knockout (Fig. 7A-C). But further immune cell subtype analysis in aged knockout mice revealed peri-islet cytotoxic T-cell accumulation (Fig. 7D-G), which are known to be a driver for β-cell destruction in diabetes-associated insulitis [60, 70, 71], and which may therefore aggravate local inflammation and compromise β-cell function.

To conclude, our findings highlight a critical difference between short-term pharmacological inhibition and lifelong genetic deletion. In aged mice short-term TLR4 blockade reduces fibrosis, insulitis, and macrophage infiltration while preserving β-cell function supporting healthy aging of the Langerhans islets. These

local structural improvements may, over a longer treatment period, also translate into measurable metabolic benefits.

In contrast, constitutive loss of TLR4 in myeloid cells, initiated before the immune and endocrine systems fully mature, appears to remove necessary developmental cues, leading to altered islet architecture, dysfunctional insulin secretion, and features of early insulin resistance. Thus, while TLR4 inhibition may be beneficial in the context of established low-grade inflammation during aging, lifelong loss of myeloid TLR4 signaling can be detrimental, particularly when initiated during development.

Acknowledgements

Graphics of Fig. 3A and Fig. 4A were created in BioRender and are available under following link: Created in BioRender. Jelleschitz, J. (2025) https://BioRender.com/eb3k0lk. This work was supported by the Deutsche Forschungsgemeinschaft (DFG, German Research Foundation; Grant HO 5332/4-1 to AH), the German Center for Diabetes Research (DZD; Grant 82DZD0034G), and the Austrian Science Fund (FWF; Grant I04844 to IB).

Author Contributions

Conception and experimental design: A.B., I.B., A.H. Funding acquisition and supervision: I.B, A.H. Formal Analysis: J.J. Interpretation: J.J., A.H. Investigation and Methodology: J.J., A.B., K.B, V.S, T.J. Writing – Original Draft: J.J., A.H, Writing – Review & Editing: J.J, A.H, I.B., A.B.

Competing Interests

The authors declare that they have no competing interests.

Data and Materials Availability

The datasets used and/or analyzed during the current study are available from the corresponding author on reasonable request.

Supplementary Materials

The Supplementary data can be found online at: www.aginganddisease.org/EN/10.14336/AD.2025.1130.

References

[1] Santoro A, Bientinesi E, Monti D (2021). Immunosenescence and inflammaging in the aging process: age-related diseases or longevity? Ageing Res Rev, 71:101422.

[2] Batista MA, Calvo-Fortes F, Silveira-Nunes G, Camatta GC, Speziali E, Turroni S, et al. (2020). Inflammaging in Endemic Areas for Infectious Diseases. Front Immunol, 11:579972.

[3] Xia S, Zhang X, Zheng S, Khanabdali R, Kalionis B, Wu J, et al. (2016). An Update on Inflamm-Aging: Mechanisms, Prevention, and Treatment. J Immunol Res, 2016:8426874.

[4] Bommer C, Sagalova V, Heesemann E, Manne-Goehler J, Atun R, Bärnighausen T, et al. (2018). Global Economic Burden of Diabetes in Adults: Projections From 2015 to 2030. Diabetes Care, 41:963-970.

[5] Ong KL, Stafford LK, McLaughlin SA, Boyko EJ, Vollset SE, Smith AE, et al. (2023). Global, regional, and national burden of diabetes from 1990 to 2021, with projections of prevalence to 2050: a systematic analysis for the Global Burden of Disease Study 2021. Lancet, 402:203-234.

[6] Bellary S, Kyrou I, Brown JE, Bailey CJ (2021). Type 2 diabetes mellitus in older adults: clinical considerations and management. Nat Rev Endocrinol, 17:534-548.

[7] Zhu M, Liu X, Liu W, Lu Y, Cheng J, Chen Y (2021). β cell aging and age-related diabetes. Aging (Albany NY), 13:7691-7706.

[8] Hill TG, Hill DJ (2024). The Importance of Intra-Islet Communication in the Function and Plasticity of the Islets of Langerhans during Health and Diabetes. Int J Mol Sci, 25:4070.

[9] Denroche HC, Miard S, Sallé-Lefort S, Picard F, Verchere CB (2021). T cells accumulate in non-diabetic islets during ageing. Immun Ageing, 18:8.

[10] Jelleschitz J, Heider S, Kehm R, Baumgarten P, Ott C, Schnell V, et al. (2025). Insulitis and aging: Immune cell dynamics in Langerhans islets. Redox Biol, 82:103587.

[11] Murao N, Yokoi N, Takahashi H, Hayami T, Minami Y, Seino S (2021). Increased glycolysis affects β-cell function and identity in aging and diabetes. Mol Metab, 55:101414.

[12] Ying W, Fu W, Lee YS, Olefsky JM (2020). The role of macrophages in obesity-associated islet inflammation and β-cell abnormalities. Nat Rev Endocrinol, 16:81-90.

[13] Ehses JA, Böni-Schnetzler M, Faulenbach M, Donath MY (2008). Macrophages, cytokines and beta-cell death in Type 2 diabetes. Biochem Soc Trans, 36:340-342.

[14] Ehses JA, Perren A, Eppler E, Ribaux P, Pospisilik JA, Maor-Cahn R, et al. (2007). Increased Number of Islet-Associated Macrophages in Type 2 Diabetes. Diabetes, 56:2356-2370.

[15] Eguchi K, Manabe I (2013). Macrophages and islet inflammation in type 2 diabetes. Diabetes Obes Metab, 15 Suppl 3:152-158.

[16] Li J, Chen L, Zhang Y, Zhang W, Xu W, Qin Y, et al. (2013). TLR4 is required for the obesity-induced pancreatic beta cell dysfunction. Acta Biochim Biophys Sin (Shanghai), 45:1030-1038.

[17] Chittezhath M, Wai C, Tay V, Chua M, Langley S, Ali Y (2020). TLR4 signals through islet macrophages to

alter cytokine secretion during diabetes. J Endocrinol, 247:87.
[18] Ladefoged M, Buschard K, Hansen A (2013). Increased expression of toll-like receptor 4 and inflammatory cytokines, interleukin-6 in particular, in islets from a mouse model of obesity and type 2 diabetes. APMIS, 121:531-538.
[19] Kawai T, Akira S (2007). TLR signaling. Semin Immunol, 19:24-32.
[20] Akira S, Uematsu S, Takeuchi O (2006). Pathogen Recognition and Innate Immunity. Cell, 124:783-801.
[21] Jin C, Baumann A, Brandt A, Engstler A, Nier A, Hege M, et al. (2020). Aging-related liver degeneration is associated with increased bacterial endotoxin and lipopolysaccharide binding protein levels. Am J Physiol Gastrointest Liver Physiol, 318:G736-G747.
[22] Baumann A, Hernández-Arriaga A, Brandt A, Sánchez V, Nier A, Jung F, et al. (2021). Microbiota profiling in aging-associated inflammation and liver degeneration. Int J Med Microbiol, 311:151500.
[23] Bergheim I, Moreno-Navarrete J (2024). The relevance of intestinal barrier dysfunction, antimicrobial proteins and bacterial endotoxin in metabolic dysfunction-associated steatotic liver disease. Eur J Clin Invest, 54:e14224.
[24] Spruss A, Kanuri G, Wagnerberger S, Haub S, Bischoff SC, Bergheim I (2009). Toll-Like Receptor 4 Is Involved in the Development of Fructose-Induced Hepatic Steatosis in Mice. Hepatology, 50:1094-1104.
[25] Kehm R, Jahnert M, Deubel S, Flore T, Konig J, Jung T, et al. (2020). Redox homeostasis and cell cycle activation mediate beta-cell mass expansion in aged, diabetes-prone mice under metabolic stress conditions: Role of thioredoxin-interacting protein (TXNIP). Redox Biol, 37:101748.
[26] Kehm R, König J, Nowotny K, Jung T, Deubel S, Gohlke S, et al. (2018). Age-related oxidative changes in pancreatic islets are predominantly located in the vascular system. Redox Biol, 15:387-393.
[27] Lee E, Ryu GR, Ko S-H, Ahn Y-B, Yoon K-H, Ha H, et al. (2011). Antioxidant treatment may protect pancreatic beta cells through the attenuation of islet fibrosis in an animal model of type 2 diabetes. Biochem Biophys Res Commun, 414:397-402.
[28] Hayden MR, Patel K, Habibi J, Gupta D, Tekwani SS, Whaley-Connell A, et al. (2008). Attenuation of Endocrine-Exocrine Pancreatic Communication in Type 2 Diabetes: Pancreatic Extracellular Matrix Ultrastructural Abnormalities. J Cardiometab Syndr, 3:234-243.
[29] Gregori S, Giarratana N, Smiroldo S, Uskokovic M, Adorini L (2002). A 1α,25-Dihydroxyvitamin D3 Analog Enhances Regulatory T-Cells and Arrests Autoimmune Diabetes in NOD Mice. Diabetes, 51:1367-1374.
[30] Lundberg M, Seiron P, Ingvast S, Korsgren O, Skog O (2017). Insulitis in human diabetes: a histological evaluation of donor pancreases. Diabetologia, 60:346-353.
[31] Jung F, Burger K, Staltner R, Brandt A, Mueller S, Bergheim I, et al. (2021). Markers of Intestinal Permeability Are Rapidly Improved by Alcohol Withdrawal in Patients with Alcohol-Related Liver Disease. Nutrients, 13:1659.
[32] Nier A, Engstler AJ, Maier IB, Bergheim I (2017). Markers of intestinal permeability are already altered in early stages of non-alcoholic fatty liver disease: Studies in children. PLoS One, 12:e0183282.
[33] Brandt A, Baumann A, Hernández-Arriaga A, Jung F, Nier A, Staltner R, et al. (2022). Impairments of intestinal arginine and NO metabolisms trigger aging-associated intestinal barrier dysfunction and 'inflammaging'. Redox Biol, 58:102528.
[34] Sovran B, Hugenholtz F, Elderman M, Van Beek AA, Graversen K, Huijskes M, et al. (2019). Age-associated Impairment of the Mucus Barrier Function is Associated with Profound Changes in Microbiota and Immunity. Sci Rep, 9:1437.
[35] Morris D (2015). Minireview: Emerging Concepts in Islet Macrophage Biology in Type 2 Diabetes. Mol Endocrinol, 29:946-962.
[36] Janssen JAMJL (2021). Hyperinsulinemia and Its Pivotal Role in Aging, Obesity, Type 2 Diabetes, Cardiovascular Disease and Cancer. Int J Mol Sci, 22:7797.
[37] Ling C (2020). Epigenetic regulation of insulin action and secretion - role in the pathogenesis of type 2 diabetes. J Intern Med, 288:158-167.
[38] He W, Rebello O, Savino R, Terracciano R, Schuster-Klein C, Guardiola B, et al. (2019). TLR4 triggered complex inflammation in human pancreatic islets. Biochim Biophys Acta Mol Basis Dis, 1865:86-97.
[39] Mohammad S, Thiemermann C (2021). Role of Metabolic Endotoxemia in Systemic Inflammation and Potential Interventions. Front Immunol, 11:594150.
[40] Patterson E, Ryan PM, Cryan JF, Dinan TG, Ross RP, Fitzgerald GF, et al. (2016). Gut microbiota, obesity and diabetes. Postgrad Med J, 92:286-300.
[41] Dula S, Jecmenica M, Wu R, Jahanshahi P, Verrilli G, Carter J, et al. (2010). Evidence that low-grade systemic inflammation can induce islet dysfunction as measured by impaired calcium handling. Cell Calcium, 48:133-142.
[42] O'Neill C, Lu C, Corbin K, Sharma P, Dula S, Carter J, et al. (2013). Circulating levels of IL-1B+IL-6 cause ER stress and dysfunction in islets from prediabetic male mice. Endocrinology, 154:3077-3088.
[43] Lilly AC, Astsaturov I, Golemis EA (2023). Intrapancreatic fat, pancreatitis, and pancreatic cancer. Cell Mol Life Sci, 80:206.
[44] Amyot J, Semache M, Ferdaoussi M, Fontés G, Poitout V (2012). Lipopolysaccharides Impair Insulin Gene Expression in Isolated Islets of Langerhans via Toll-Like Receptor-4 and NF-κB Signalling. PLoS One, 7:e36200.
[45] Matsunaga N, Tsuchimori N, Matsumoto T, Ii M (2011). TAK-242 (resatorvid), a small-molecule inhibitor of Toll-like receptor (TLR) 4 signaling, binds selectively to TLR4 and interferes with interactions between TLR4 and its adaptor molecules. Mol Pharmacol, 79:34-41.

[46] Takashima K, Matsunaga N, Yoshimatsu M, Hazeki K, Kaisho T, Uekata M, et al. (2009). Analysis of binding site for the novel small-molecule TLR4 signal transduction inhibitor TAK-242 and its therapeutic effect on mouse sepsis model. Br J Pharmacol, 157:1250-1262.

[47] Zhang N, Liang H, Farese R, Li J, Musi N, Hussey S (2015). Pharmacological TLR4 Inhibition Protects against Acute and Chronic Fat-Induced Insulin Resistance in Rats. PLoS One, 10:e0132575.

[48] Liang H, Hussey S, Sanchez-Avila A, Tantiwong P, Musi N (2013). Effect of lipopolysaccharide on inflammation and insulin action in human muscle. PLoS One, 8:e63983.

[49] Liu S, Wu J, Chen P, Mohammed S, Zhang J, Liu S (2022). TAK-242 Ameliorates Hepatic Fibrosis by Regulating the Liver-Gut Axis. Biomed Res Int, 2022:4949148.

[50] Bhattacharyya S, Wang W, Tamaki Z, Shi B, Yeldandi A, Tsukimi Y, et al. (2018). Pharmacological Inhibition of Toll-Like Receptor-4 Signaling by TAK242 Prevents and Induces Regression of Experimental Organ Fibrosis. Front Immunol, 9:2434.

[51] Apte M, Haber P, Darby S, Rodgers S, McCaughan G, Korsten M, et al. (1999). Pancreatic stellate cells are activated by proinflammatory cytokines: implications for pancreatic fibrogenesis. Gut, 44:534-541.

[52] Mews P, Phillips P, Fahmy R, Korsten M, Pirola R, Wilson J, et al. (2002). Pancreatic stellate cells respond to inflammatory cytokines: potential role in chronic pancreatitis. Gut, 50:535-541.

[53] Tschen S, Dhawan S, Gurlo T, Bhushan A (2009). Age-dependent decline in beta-cell proliferation restricts the capacity of beta-cell regeneration in mice. Diabetes, 58:1312-1320.

[54] Taschetto APD, Zimath PL, Silvério R, Santos Cd, Boschero AC, Santos GJd, et al. (2021). Reduced insulin sensitivity and increased β/α cell mass is associated with reduced hepatic insulin-degrading enzyme activity in pregnant rats. Life Sci, 277:119509.

[55] Protzek AOP, Rezende LF, Costa-Júnior JM, Ferreira SM, Cappelli APG, Paula FMMd, et al. (2016). Hyperinsulinemia caused by dexamethasone treatment is associated with reduced insulin clearance and lower hepatic activity of insulin-degrading enzyme. J Steroid Biochem Mol Biol, 155:1-8.

[56] Farris W, Mansourian S, Chang Y, Lindsley L, Eckman EA, Frosch MP, et al. (2003). Insulin-degrading enzyme regulates the levels of insulin, amyloid β-protein, and the β-amyloid precursor protein intracellular domain in vivo. Proc Natl Acad Sci U S A, 100:4162-4167.

[57] Tudurí E, Soriano S, Almagro L, García-Heredia A, Rafacho A, Alonso-Magdalena P, et al. (2022). The Effects of Aging on Male Mouse Pancreatic β-Cell Function Involve Multiple Events in the Regulation of Secretion: Influence of Insulin Sensitivity. J Gerontol A Biol Sci Med Sci, 77:405-415.

[58] Böni-Schnetzler M, Ehses M, Faulenbach JA, Donath MY (2008). Insulitis in type 2 diabetes. Diabetes Obes Metab, 10 Suppl 4:201-204.

[59] Campbell-Thompson M, Fu A, Kaddis JS, Wasserfall C, Schatz DA, Pugliese A, et al. (2016). Insulitis and β-Cell Mass in the Natural History of Type 1 Diabetes. Diabetes, 65:719-731.

[60] Morgan NG (2024). Insulitis in human type 1 diabetes: lessons from an enigmatic lesion. Eur J Endocrinol, 190:R1–9.

[61] Nikolic T, Geutskens SB, Rooijen Nv, Drexhage HA, Leenen PJM (2005). Dendritic cells and macrophages are essential for the retention of lymphocytes in (peri)-insulitis of the nonobese diabetic mouse: a phagocyte depletion study. Lab Invest, 85:487-501.

[62] Jansen A, Homo-Delarche F, Hooijkaas H, Leenen P, Dardenne M, Drexhage H (1994). Immunohistochemical characterization of monocytes-macrophages and dendritic cells involved in the initiation of the insulitis and beta-cell destruction in NOD mice. Diabetes, 43:667-675.

[63] Vaure CL, Liu Y (2014). A Comparative Review of Toll-Like Receptor 4 Expression and Functionality in Different Animal Species. Front Immunol, 5:316.

[64] Nagaraj V, Kazim AS, Helgeson J, Lewold C, Barik S, Buda P, et al. (2016). Elevated Basal Insulin Secretion in Type 2 Diabetes Caused by Reduced Plasma Membrane Cholesterol. Mol Endocrinol, 30:1059-1069.

[65] Gülden E, Ihira M, Ohashi A, Reinbeck AL, Freudenberg MA, Kolb H, et al. (2013). Toll-Like Receptor 4 Deficiency Accelerates the Development of Insulin-Deficient Diabetes in Non-Obese Diabetic Mice. PLoS One, 8:e75385.

[66] Yan S, Jiang Z, Cheng L, Lin Y, Fan B, Luo L, et al. (2020). TLR4 knockout can improve dysfunction of β-cell by rebalancing proteomics disorders in pancreas of obese rats. Endocrine, 67:67-79.

[67] Cao Y, Han X, Wang Z, Liu Y, Wang Y, Zhang R, et al. (2021). TLR4 knockout ameliorates streptozotocin-induced osteoporosis in a mouse model of diabetes. Biochem Biophys Res Commun, 546:185-191.

[68] Zinselmeyer BH, Vomund AN, Saunders BT, Johnson MW, Carrero JA, Unanue ER (2018). The resident macrophages in murine pancreatic islets are constantly probing their local environment, capturing beta cell granules and blood particles. Diabetologia, 61:1374-1383.

[69] Cosentino C, Regazzi R (2021). Crosstalk between Macrophages and Pancreatic β-Cells in Islet Development, Homeostasis and Disease. Int J Mol Sci, 22:1765.

[70] Pugliese A (2016). Insulitis in the pathogenesis of type 1 diabetes. Pediatr Diabetes, 17 Suppl 22:31-36.

[71] In'T Veld P (2014). Insulitis in human type 1 diabetes: a comparison between patients and animal models. Semin Immunopathol, 36:569-579.